International Congress of Science and Technology of Metallurgy and Materials, SAM - CONAMET 2013

β-grain size effects on the 18R-martensite microstructure in Cu-based SMA

P. La Roca[a], L. Isola[a], Ph. Vermaut[b], J. Malarría[a]*

[a] Instituto de Física Rosario (CONICET-Universidad Nacional de Rosario) Bvrd. 27 de Febrero 210 Bis, S2000EZP, Rosario, Argentina
[b] Laboratoire de Métallurgie Structurale, Ecole Nationale Superieure de Chimie de Paris, 11 rue Pierre et Marie Curie, 75231 Paris Cedex 5, France

Abstract

A systematic experimental analysis based on the assessment of the mean martensite plate size in sub-grain domains was implemented to characterize the martensitic microstructure morphology in polycrystalline Cu-based shape memory alloys. Experimental data was collected by light and electron microscopy, analysing polycrystalline materials of grain size (d) in a wide range: from fine-grained material with grain size of about 500 nm (ribbons and strips obtained by rapid solidification techniques) to single crystals of 6 mm diameter (grown by the Bridgman method). In the d range below 100 μm, a lineal relationship between the average width of the martensite plates (h_{plate}) and the mean grain size was obtained for thermal-induced martensite transformation (*TMT*). Above this value ($d > 100$ μm), such relation is no longer valid, and h_{plate} becomes independent of grain size.

Nomenclature

SMA shape memory alloy
M_s martensitic transformation start temperature
D mean characteristic length of the grain size
h_{plate} average width of the martensite plates

---

* Corresponding author. Tel.: +54 341 485 3200; fax: +54 341 480 8584.
E-mail address: malarria@ifir-conicet.gov.ar.

1. Introduction

In shape memory alloys (SMA), the grain size (*d*) can be reduced in order to improve the mechanical properties (Sure and Brown [1984]). This is effective, for instance, to reduce fragility in the SMA *Cu*-based alloys, although the grain size reduction yields a change in the transformation temperatures. This effect was pointed out by a large number of authors. It has been shown that for *d* greater than 100 µm, the start temperature of the martensitic transformation (M_s) is generally independent of *d*. However, the M_s decreases when *d* is reduced below 100 µm. This behaviour was observed in different shape memory polycrystalline alloys: *Fe-Ni-C* (Hayzelden and Cantor [1986]), *Fe-Pd* (Seki et al. [2008]), *Cu-Zn-Al* (Jianxin et al. [1988a]; Adnyana [1986]), *Cu-Al-Ni* (Mukunthan and Brown [1989]) and *Cu-Al-Mn* (López del Castillo et al. [1987]).

There are other phenomena related with grain size, which can affect the transformation and material properties. When the phase transformation happens, the austenite grain size reduction yields a martensitic morphology with smaller plate size (Porter et al. [2009]; Shibata et al. [2012]). In the seventies, this phenomenon had some impact in the scientific community because it was discovered a Hall-Petch relation between the yield stress and the martensitic plate width (Khan et al. [1970, 1974]). Therefore, the material yield stress is increased through the decrease of the martensitic plate width (Khan and Delaey [1970]). In the work (Khan [1974]), a relation between grain and plate size as $h_{plate} \alpha d^{1/3}$ was obtained by fitting experimental data in a limited range of the grain size. Also, in low carbon steel, the martensitic plate size reduction has an important influence in the resistance to fracture or perforation due to ballistic impact (Maweja et al. [2009]).

On the other hand, in the last ten years the SMA community has concentrated efforts in the study of the "size effects" (Waitz and Karnthaler [2004]; Chen and Schuh [2011]; Ozdemir et al. [2012]). They are consequence of the reduction of the different macro or microstructure characteristic parameters of the material, like grain size, micro-wire diameter, thin film thickness or particle size. The implications of these effects over the superelasticity and shape memory behaviour has gained more interest due to the potential use of these materials in small scale devices (Kohl et al. [2006]; Tomozawa et al. [2010]; Barth et al. [2010]).

For instance, in nanostructured *Ni-Ti*, the grain size effect in the thermal-induced martensitic transformation has been investigated (Waitz et al. [2004, 2007]). It was found that the martensitic transformation is completely suppressed when the grain size is reduced below 50 nm. This effect was explained by the presence of an energy barrier related to the martensite-martensite (m-m) interface energy, the surface energy strain and austenite-martensite interface energy. In the work (Waitz et al. [2007]), a relation $h_{plate} \propto d^{1/2}$ was used to assess the m-m interface energy change when *d* is reduced.

Moreover, the martensitic plate size and the *m-m* interface energy are very important parameters for theoretical models, which try to describe the SMA behaviour when the size effects are present (Waitz et al. [2007]; Petryk and Stupkiewicz [2010]; Petryk et al. [2010]).

To gain new insights in understanding the role of size effects in Cu-based shape memory materials, a systematic experimental study of the relation between *d* and h_{plate} is presented in large *d* range from 500 nm to 6 mm.

2. Experimental Set-up

In order to perform a study of a wide range of the grain size, different production techniques and thermal treatments were performed. Rapid solidification techniques allow us to obtain polycrystalline material with grain size lower than the produced by conventional techniques. For example, Melt Spinning (MS) and Twin Roll Casting (TRC) were successfully applied in *Cu*-based SMA to develop samples with grain size lower than 500 nm (Dutkiewicz et al. [1999]; Font et al. [2003]; Malarría et al. [2006, 2009]; Sobrero et al. [2008]).

In this work, ribbons (~ 50 µm in thickness) and strips (~ 300 µm in thickness) were produced by MS and TRC, respectively. The processing parameters, the alloy chemical compositions and the mean grain size of the sample are presented in Table 1. In order to modify the as-cast grain size, different samples were annealed at 700°C, 800°C and 900°C during 30 minutes, and then they were quenched in water-ice solution. A second thermal treatment was performed at 200°C during 15 minutes followed by air cooling, to release stress, promote the order and remove the excess vacancies (Somerday et al. [1997]). Thereby, samples with a wide range of *d*, between 1 µm and 100 µm, were obtained.

Table 1. Samples produced by rapid solidification techniques. Casting parameters.

Sample	Alloys [at. %]	Tech.	V_{roll} [m/s]	$P_{eject.}[mbar]$	$T_{melt}[°C]$	d [μm]
89	*Cu*-13 *Al*-5 *Ni*	MS	19	250	1370	3
55	*Cu*-13 *Al*-5.5 *Ni*-1*Ti*	MS	19	250	1385	1-2
*D*1	*Cu*-13 *Al*-5 *Ni*	TRC	0.6	250	1170	24
*R*10	*Cu*-13 *Al*-6 *Ni*-1*Ti*	TRC	0.84	250	1150	5

On the other hand, different pieces of a *Cu*-13*Al*-5*Ni*-(0.5*Ti*-0.1*Cr*) at.% wire were re-melted and solidified at different cooling speeds (SDCS) to promote different microstructural conditions, with *d* between 100 μm and 1 mm (see table 2).

In order to complete the crystal range upper than 1 mm, single-crystals of *Cu-Al-Ni* produced by Bridgman method (BM), were machined in cylindrical shapes of 2, 4 and 6 mm diameters (see table 2).

Table 2. Coarse grain samples and single crystals.

Sample	Alloys [at. %]	Technique	d [μm]
89	*Cu*-13 *Al*-5 *Ni*	SDCS	100-1000
55	*Cu*-13 *Al*-5.5 *Ni*-1*Ti*	BM	2000
*D*1	*Cu*-13 *Al*-5 *Ni*	BM	4000
*R*10	*Cu*-13 *Al*-6 *Ni*-1*Ti*	BM	6000

Due to the alloys compositions, all samples present transformation temperatures over the room temperature, so all of them are in the 18*R* martensitic phase at this temperature.

To perform proper measurements of h_{plate} and *d*, it was necessary to take a large number of sample images to obtain reliable statistical results.

The microstructure of the samples with *d* > 10 μm was observed with Olympus PM3 optical microscope using Nomarski interference contrast. These samples were electro-polisher with $20\%H_2SO_4$-$47\%H_3PO_4$-H_2O during 30 second at 8 V and 5 °C. The samples with lower *d* were analyzed by a Philips EM300 transmission electron microscope (TEM) and the thin foils were prepared with twin-jet electro-polisher using $30\%HNO_3$-metanol as solution at $T = -10$ °C.

3. Measurement procedures of h_{plate} and d

In order to outline a relation between *d* and h_{plate}, these magnitudes were measured in different grains observed in TEM and optical images. The *d* was calculated averaging the maximum (d_{max}) and the minimum diameters (d_{min}), that is:

$$d = (d_{max} + d_{min})/2 \tag{1}$$

In most of the grains, more than one parallel plate domain was observed in the martensitic structure and also the self-accommodation structure (see figure 1(a)). Thus, it was necessary to introduce a measurement method to determine h_{plate}.
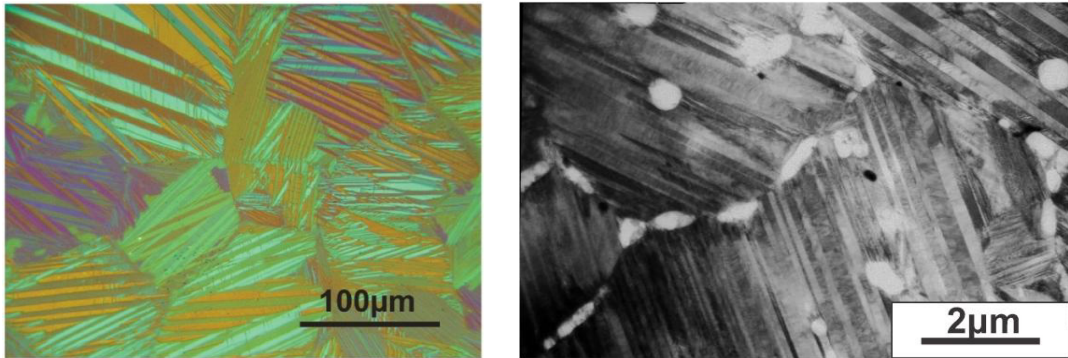
Fig. 1. (a) Optical micrography, (b) TEM bright field image.

This method consists in drawing a normal line to the parallel plates in each domain (see Figure 2). The line length (S_i) was taken as the characteristic dimension of the martensitic domain and the number of intersections (N_i) was determined. Then, h_{plate} of a given grain was calculated averaging the mean value of the martensitic plate size of each domain, weighted by S_i. That is:

$$h_{plate} = \frac{1}{S_{tot}} \sum_{i=1}^{n} S_i \frac{S_i}{N_i+1} \quad \text{where} \quad S_{tot} = \sum_{i=1}^{n} S_i \tag{2}$$

These measures were performed in more than 30 images and 250 grains of different sizes.
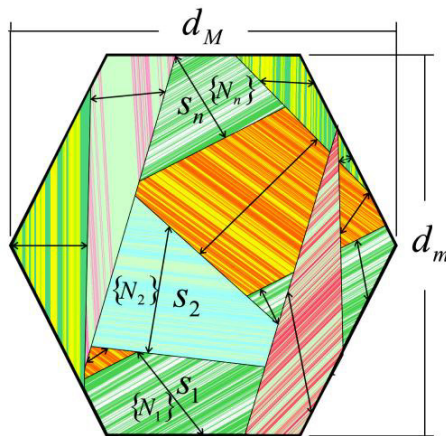

Fig. 2. The measurement method of h_{plate}.

4. Results and Discussion

4.1. Experimental determination of the relationship between h_{plate} and d

Figures 1(a) and 1(b) are optical and TEM images respectively and they show the sample microstructures with different grain sizes. In Figure 1(a), it can be observed the different orientations of the martensitic parallel plates in each domain inside the grains. It is interesting to note that in most of the grains smaller than 10 µm there is only one domain of parallel plates (see figure 1(b)). This is similar to what was found in NiTi nano-grains, where the "herringbone" type of martensitic morphologies were not observed anymore for grains with *d* below certain value

leading to an array of parallel plates. Figure 2 is a schematic illustration to show the method adopted to determine h_{plate} (Waitz and Karnthaler [2004]).

The relation between d and h_{plate} is plotted in Figure 3 in logarithmic scale. Each point represents the average sizes measured in a grain of a given sample.

Figure 3 shows that h_{plate} is independent of grain sizes for $d > 100$ µm. However, a strong decrease of h_{plate} is observed as d is reduced below 100µm. This behavior is due to the difficulty to develop the transformation in reduced domains. So, the mean plate size is decreased to have more geometric possibilities to accommodate the transformation strain and match the structure at the grain boundaries.
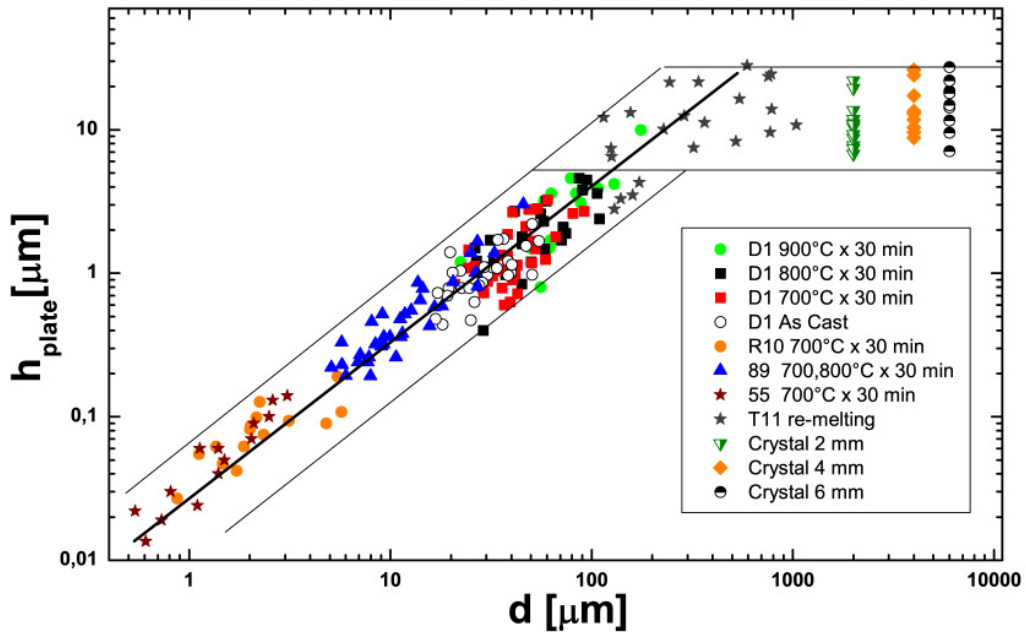

Fig. 3. Experimental measurements of h_{plate} as a function of d.

In order to find a functional relation between these parameters, the experimental data was fitted, in the range of d below 100µm, by the potential function $h_{plate}(d) = A\, d^B$, where A and B are the fit parameters. The function was fitted using the least square method on the logarithmic value s of the measured points. The parameter values were $A=(0,036\pm0,002)$ and $B=(0,99\pm0,02)$. It is interesting to note that the B parameter is very close to 1, so it can be assumed that there is a lineal relation between h_{plate} and d. Therefore, it can be concluded that the relation between these two characteristic sizes is:

$$h_{plate}\ d\ = 0.036\, d \qquad (3)$$

This lineal relation was early suggested by Perkins [1982], he observed the same h_{plate}-d relationship in two images with very different grain sizes, like a "scale effect". However, this lineal relationship disagrees with the potential functions reported in previous works: (Khan [1974]) and (Waitz et al. [2007]). In the former work, the potential relationship was carried out fitting experimental data in a d range limited between 250 and 5000 µm, well above the range examined here. Whereas, the latter work obtained a relation $h_{plate} \propto d^{1/2}$ based on the theoretical energy minimization criterion, which agrees with their experimental measure of these magnitudes in a nanograin ($d=50$nm and $h_{plate}=2.0\pm0.5$nm). It should be mentioned that this experimental measure of the nanograins morphology is consistent with the expression (3).

It is interesting to note that the *break-point* of the behavior plotted in Figure 3 occurs at $d = 100$ μm. This is consistent with the fact that the M_s decreases, when d is reduced below 100 μm (Adnyana [1986]; Jianxin et al. [1988b]; Mukunthan and Brown [1989]; Dutkiewicz et al. [1999]). This agreement supports the idea that the size has already an effect below this d value in the martensitic transformations.

The relation between h_{plate} and d (expression (3)) can be understood through energy minimization criterion, when the martensitic transformation is carried out under a grain boundary constrain. Each martensitic variant has a given transformation strain associated to it and it is necessary to accommodate these strains to the grain boundary structure. So, in order to minimize the strain at grain boundary, the number of variants involved in the transformation is increased as the grains size is reduced. Then, the greater number of variant will be related to the decrease of h_{plate}.

Note that the reduction of h_{plate} yields an increase of the m-m interface density per unit volume. Although that commonly the energies of these interfaces are very small, when the grain size is reduced, the total *m-m* interface energy could be large due to the growth of the interface *m-m* density. The stabilization of the austenite phase by this energy barrier was already observed in nanostructured Ni-Ti alloys (Waitz et al. [2007]).

5. Conclusion

Through a systematic experimental method based on the evaluation of the plate size in domains, a relationship between the average width plate and grains size was obtained ($h_{plate}(d) = 0.036\ d$). This experimental relationship is useful as input parameter of theoretical models, which study size effects in martensitic transformation.

Acknowledgements

References

Adnyana, D.N., 1986. Effect of grain size on transformation temperatures in a grain-refined copper-based, shape-memory alloy. Metallography 19, 1986.

Barth, J., Krevet, B., Kohl, M., 2010. A bistable shape memory microswitch with high energy density. Smart Materials and Structures 19, 094004.

Chen, Y., Schuh, C.A., 2011. Size effects in shape memory alloy microwires. Acta Materialia 59, 537–553.

Dutkiewicz, J., Czeppe, T., Morgiel, J., 1999. Effect of titanium on structure and martensic transformation in rapidly solidified CuAlNiMnTi alloys. Materials Science and Engineering A 275, 703 – 707.

Font, J., Cesari, E., Muntasell, J., Pons, J., 2003. Thermomechanical cycling in Cu-Al-Ni-based melt-spun shape memory ribbons. Materials Science and Engineering A 354, 207–211.

Hayzelden, C., Cantor, B., 1986. The martensite transformation in Fe-Ni-C alloys. Acta Metallurgica 34, 233–242.

Jianxin, W.U., Bohong, J., Hsu, T., 1988a. Influence of grain size and ordering degree of the parent phase on Ms in a Cu-Zn-Al alloy containing boron. Acta Metallurgica 36, 1521–1526.

Khan, A., 1974. The application and interpretation of the "time law " to the growth of grain size and martensite plate thickness in copper-based martensites. Journal of Materials Science (full set) 9, 1290–1296.

Khan, A., Brabers, M., Delaey, L., 1974. The Hall-Petch relationship in copper-based martensites. Materials Science & Engineering A 15, 263–274.

Khan, A., Delaey, L., 1970. The martensite-plate-size dependence of yield strength of copper-aluminium-zinc martensite. Scripta Metallurgica 4, 981–984.

Khan, A., Delaey, L., Tas, H., Lefever, I., Vos, L.,Meester, L., Deruyttere, A., DeMeester, P., 1970. The mechanical properties of copper-aluminium bronzes. Proceedings of the 2nd International Conference on the Strength of Metals and Alloys.

Kohl, M., Agarwal, a., Chernenko, V., Ohtsuka, M., Seemann, K., 2006. Shape memory effect and magnetostriction in polycrystalline NiMnGa thin film microactuators. Materials Science and Engineering: A 438-440, 940–943.

López del Castillo, C., Mellor, B., Blázquez, M., Gómez, C., 1987. The influence of composition and grain size on the martensitic transformation temperatures of Cu-Al-Mn shape memory alloys. Scripta Metallurgica 21, 90163.

Malarría, J., Elgoyhen, C., Vermaut, P., Ochin, P., Portier, R., 2006. Shape memory properties of Cu-based thin tapes obtained by rapid solidificationn methods. Materials Science and Engineering A 440, 763–767.

Malarría, J., La Roca, P., Vermaut, P., Ochin, P., Portier, R., 2009. Cu-based shape memory strips elaborated by one-step rapid solidification techniques: structural and functional properties, in: 11th Internacional Conference on Advanced Materials, Rio de Janiro, Brasil.

Maweja, K., Stumpf,W., van der Berg, N., 2009. Characteristics of martensite as a function of the Ms temperature in low-carbon armor steel plates. Materials Science and Engineering: A 519, 121–127.

Mukunthan, K., Brown, L., 1989. Preparation and Properties of Fine Grain Cu-AI-Ni Strain Memory Alloys. Metallurgical Transactions A 11, 90505.

Ozdemir, N., Karaman, I., Mara, N., Chumlyakov, Y., Karaca, H., 2012. Size effects in the superelastic response of Ni54Fe19Ga27 shape memory alloy pillars with a two stage martensitic transformation. Acta Materialia 60, 5670–5685.

Perkins, J., 1982. Rapid Solidification Effects in Martensitic Cu-Zn-AI Alloys. Metallurgical Transactions 13, 1367–1372.

Petryk, H., Stupkiewicz, S., 2010. Interfacial energy and dissipation in martensitic phase transformations. Part I: Theory. Journal of the Mechanics and Physics of Solids 58, 390–408.

Petryk, H., Stupkiewicz, S., Maciejewski, G., 2010. Interfacial energy and dissipation in martensitic phase transformations. Part II: Size effects in pseudoelasticity. Journal of the Mechanics and Physics of Solids 58, 373–389.

Porter, D., Esterling, K., Sherif, M., 2009. Phase transformations in metals and alloys. 2nd ed. ed., Chapman and Hall, London.

Seki, K., Kura, H., Sato, T., Taniyama, T., 2008. Size dependence of martensite transformation temperature in ferromagnetic shape memory alloy FePd. Journal of Applied Physics 103, 063910.

Shibata, A., Jafarian, H., Tsuji, N., 2012. Microstructure and Crystallographic Features of Martensite Transformed from Ultrafine-Grained Austenite in Fe24Ni0.3C Alloy. Materials Transactions 53, 81–86.

Sobrero, C.E., Bolmaro, R., Malarría, J., Ochin, P., Portier, R., 2008. Texture in Cu-based shape memory strips obtained by twin roll casting. Materials Science and Engineering: A 481-482, 688–692.

Somerday, M., Comstock, R.J., Wert, J.A., 1997. Effect of Grain Size on the Observed Pseudoelastic Behavior of a Cu-Zn-Al Shape Memory Alloy. Metallurgical and Materials Transactions A 28, 2335–2341.

Sure, G.N., Brown, L.C., 1984. The mechanical properties of grain refined-CuAlNi strain-memory alloys. Metallurgical Transactions A 15 A,1613–1621.

Tomozawa, M., Kim, H., Yamamoto, a., Hiromoto, S., Miyazaki, S., 2010. Effect of heat treatment temperature on the microstructure and actuation behavior of a TiNiCu thin film microactuator. Acta Materialia 58, 6064–6071.

Waitz, T., Antretter, T., Fischer, F.D., Simha, N.K., 2007. Size effects on the martensitic phase transformation of NiTi nanograins. Journal of the Mechanics and Physics of Solids 55, 419–444.

Waitz, T., Karnthaler, H.P., 2004. Martensitic transformation of NiTi nanocrystals embedded in an amorphous matrix. Acta Materialia 52, 5461-5469.

Waitz, T., Kazykhanov, V., Karnthaler, H.P., 2004. Martensitic phase transformations in nanocrystalline NiTi studied by TEM. Acta Materialia 52, 137–147.